Originally published in *Proceedings of the Fifth International Workshop on Compressible Turbulent Mixing*, ed. R. Young, J. Glimm & B. Boston.
ISBN 9810229100, World Scientific (1996).

Instability and Turbulence Triggered by a Density Perturbation on a Slab Accelerated by Thermal-Radiation-Driven Ablation

A. Caruso and V. A. Pais

Associazione Euratom - ENEA sulla Fusione
C. E. Frascati C. P. 65-00044 Frascati, Roma,
Italia

Abstract. The effect of a perturbation in density (like that observed in porous materials) on the evolution of a slab, formed by an internal layer of Deuterium-Tritium and an external layer of Aluminum, accelerated by thermal radiation ablation is being studied. A temporally-profiled thermal radiation pulse (25 ns in duration) has been used as driver for the implosion, as that expected for the case of an ICF high gain (cm sized) capsule enclosed in a hohlraum cavity. The 2D numerical simulations performed up to now, have been done on a planar analog with perturbations in density of the Aluminum layer having wavelengths in the interval 5–20 mic, initial amplitude of 0.1% and wavelength number vector oriented at 45 degrees from the slab surface. These first simulations show the growing of hydrodynamical instabilities. After a transitory period, during which the first shock wave moves through the density-perturbed Aluminum layer, leaving a spinned velocity field, the distortion of the ablation front starts to grow. Then, the evolution follows the same qualitative behaviour previously observed when the perturbation was introduced on the surface [1]. Ablation rate enhancement, turbulent fluid motion behind the shock wave, symmetry loss, hole formation in the radiation shield, fuel preheating by the thermal radiation wave, etc. are the effects again observed in the density perturbed matter evolution that may render useless the 1D based design of a high gain capsule exposed to a given thermal bath.

1 Introduction

We report here the preliminary results about the instability and the subsequent turbulence generated on a slab accelerated by ablation produced by thermal radiation, when density non-uniformities are introduced in the whole volume of the ablator/shielding layer. These density non-uniformities could appear if for example we use a porous material. As precedent works, this study derives from those on the stability of the indirect-driven scheme for the Inertial Confinement Fusion.

The study has been performed by 2D hydrodynamical simulations, using the COBI-3 Lagrangian code, whose main characteristics are:

- Three fluids: ions, electrons and photons, each one with its own temperature.
- "Real Matter" Equation-of-State.
- Thermal flux with free streaming limit.
- Radiation transport treated by a diffusive "grey" model with SESAME-fitted coefficients.
- Mesh correction by a collision technique.

The planar analog of a high gain target discussed in previous papers [2, 3, 4, 5] has been used (see Fig. 1). The choice of a planar analog is in this case justified by two circumstances:

1. The perturbation wavelengths are assumed much smaller than the target radius.
2. The phenomena of interest evolve in a time so short, that matter has no time to displace as a whole over a significant fraction of the target radius.

However, and in any case, this study remains valid for a plane geometry.

The planar analog shown in Fig. 1 corresponds to a "capsule" formed by a 120μm solid aluminum shell with a 60μm internal layer of frozen equimolar deuterium-tritium mix, the most external radius being 0.462 cm.

The "capsule" surface has been exposed to a thermal radiation field characterized by a temperature T_r depending on the time t as

$$T_r = \frac{T_{r0}}{1 - t/t_0} \quad \text{for} \quad t < 25\text{ns}. \tag{1}$$

Here, $T_{r0} = 30$eV and $t_0 = 27$ns; for $t = 25$ns the maximum radiation temperature (≈ 400eV) is achieved. Eq. 1 is a good approximation for the temperature dependence obtained in the previously quoted, 1D, high gain target simulations.

With regard to the choice of *assigning* the thermal radiation temperature instead of the injected power, we note that in the framework of this model, the absorbed power could, in principle, increase without limit as a result of a corresponding area or local thermal gradient growth.

In addition to the effects of the initial step in the assigned temperature profile (Richtmyer-Meshkov instability), a fundamental feature to be pointed out for the interpretation of the results, is the time-rising value of the temperature; due to this, the ablation pressure increases in time and the ablation surface of even an infinitely thick material will be accelerated, with important implications in terms of hydrodynamical stability.

A Cartesian framework (X, Y) was chosen with the $X-$axis playing the role of the outward radial direction and the $Y-$axis that of an azimuthal coordinate, parallel to the interfaces. The zoning used in the 2D calculations was formed by 90 cells in the $X-$direction and 40 cells/wavelength in the $Y-$direction.

The perturbation has been introduced by perturbing the cell density in the whole volume of the external Aluminum layer by a small amount given by:

$$\rho = \rho_{0,Al}\{1 + \delta \cos(\vec{k} \cdot (\vec{r} - \vec{r_0}))\} \tag{2}$$

where $\rho_{0,al}(= 2.7\text{gr/cc})$ is the unperturbed Aluminum density, $\delta(= 0.001)$ is the relative amplitude of the perturbation, $\vec{r} = (X, Y)$ points to the cell center, and $\vec{r_0} = (0.462, 0)$cm is the initial external surface position. We have kept the direction of the wavenumber vector $\vec{k}$ at 45^o with respect to the $X-$direction.

We have considered perturbations having wavelength ($\lambda = 2\pi/|\vec{k}|$) of the same order of magnitude as a characteristic scale-length of the compressed accelerated material (10μm) [3, 4, 5]. Three cases have been processed with different λ (5, 10 and 20 μm). The numerical simulation set-up described above, is shown in Fig. 2.

2 Results

The temporal evolution in all the cases has been found to be characterized by a strong hydrodynamical instability. We can describe the main features of the evolution as follows:

- After a transitory period during which the first shock wave moves through the density-perturbed Al leaving a spinned velocity field, the ablation front becomes distorted.

- The time-rising character of the temperature produces an increasing ablation pressure, an accelerated ablation front and then leads to instability, perhaps of the Rayleigh-Taylor type.

- As a consequence, the ablating surface area increases (which we have called “area effect”) and the power absorbed per unit area also increases due to local thermal gradient intensification (called “ripple effect”). So, the ablation rate and the absorbed energy grow.

- When the ablation front has become spatially distorted, the evolution follows the same kind of behaviour as the surface perturbed case.

Let us start a more detailed analysis, by first illustrating the transitory phases. Fig. 3a shows the evolution of the density during the first steps of the evolution for the 10 mic wavelength case. We can note that the front of the first shock wave seems to evolve unperturbed. However, looking at the evolution of the vorticity ($\vec{\Omega} = \frac{1}{2}\vec{\nabla} \times \vec{v}$) at the same steps (see Fig. 3b), we can see that the velocity field is highly rotational after the shock wave. This vorticity appears to cause the shock front, moving in a nonuniform density medium, to reach different velocities (and so different entropy jumps) in different points of its surface. Thus, the highly rotational velocity field promotes the deformation of the ablation front.

So, to evidence the instability growth, Fig. 4a presents the evolution of the radiation temperature at successive instants, making it possible to observe the deformation of the ablation front. In a similar way, the density perturbation grows and becomes apparent (see Fig. 4b). A point that has to be noted is that the evolution of both density and radiation temperature does not show the growth of half-wavelength modes. And it appears as the amplitude of the perturbation tends to decrease (by local thermal gradients intensification, for example). On the other hand, Fig 4c shows the growth of the vorticity field. Here, the perturbation growth is clear and the velocity field appears strongly perturbed.

To confirm this point, we can look at the subsequent evolution in which the higher harmonic modes appear, both in radiation temperature (Fig 5a) and in density (Fig 5b). In the latter figure, the "unload" of the matter due to the inward expansion, makes apparent the spinned velocity field, generating some kind of jets. This, together with the high vorticity in all the matter (Fig 5c), could generate a turbulent motion that mixes the matter and forbids the creation of the structures necessary for the ignition ("hot-spot" + dense cold matter surrounder).

3 Concluding Remarks

For the short wavelengths considered in this study, stabilization mechanisms due to ablative polishing [6], finite gradient [7] or overpressure [8] appear to be ineffectual. The case of the ablative overpressure stabilization should arise as a result of a fractional increase of the thermal flux of the ripple's maxima, this being estimated of the order $k\xi$. Actually, violent overpressure effects are observed when ξ is already of the order of λ, the main result being the transformation of the maximum in a minimum and the generation of harmonics of the initial k.

For long wavelengths, the penetration of a thermal radiation wave into the fluid may occur before the end of the temperature pulse. The process of the premature fuel preheating, by hole formation in the shield, is due to two concurrent effects. One of these is the enhancement of the ablation process. The other effect, contributing to the formation of holes, is due to the important transverse motion and matter pile-up induced in the shield by the non-linear growth of the instability; when this happens, a substantial deformation of the DT-Al interface occurs.

With regard to the evolution of Ω, it may be interesting to point out that, as when in adiabatic flows Ω is frozen in the matter, a further increase of Ω has to be expected in all the compression stages of the flow evolution (say $\Omega \sim \rho^{-2/3}$).

As noted in the introduction, the model adopted here, based on an assigned time dependent temperature at the system boundary, may allow an unlimited energy absorption as a result of area increase and "ripple effect". It is however reasonable to expect that, when instability enhanced absorption occurs to such a level to make the confinement parameter of the order of unity, the ablation process will adjust in such a way to make consistent this value with the injected external power.

4 Conclusions

Concluding, we can say that the evolution of nonuniform density layers exposed to time-tailored-temperature radiation pulses, as that given by Eq 1, is highly unstable. Even density perturbation amplitudes as small as one-tenth percent can generate very nonuniform motion and a high loss of symmetry.

The evolution is characterized by a transitory period during which the ablation front distorts and leaves a strongly perturbed velocity field followed by an evolution similar to the surface-perturbed case.

The absorbed energy and the ablation rate are enhanced due to the increase of the exposed area and the local thermal gradient intensification.

The effectiveness of such stabilizing mechanisms as ablative polishing, finite gradient or overpressure, has not been observed.

Finally, the behavior of material surfaces exposed to time-tailored temperature radiation pulses may be very different from that predicted in the 1D calculations

5 Appendix

During the congress, B. A. Remington suggested testing an already published case [9] of a CH slab of 50 μm width exposed to a time-profile-temperature radiation pulse like that obtained experimentally in a cavity irradiated with two NOVA beams. In this case, when a spatial perturbation is applied on the exposed surface of the slab, with initial amplitude $\eta_0 = 2.4\mu$m and wavelength $\lambda = 100\mu$m, the evolution of the instability shows some degree of stabilization.

We have tried the same case, but introducing a density perturbation (Eq 2 with initial amplitude $\delta = 0.001$ and wavelength $\lambda = 100\mu$m on the whole slab. The results can be seen in Fig 6 that shows the density evolution. It is apparent that the perturbation tends to vanish, leading to a sort of stabilization.

The conclusion is that using the above mentioned time-tailored-temperature radiation pulse on a relative soft material as CH, stabilization can be reached. However, the question remains on the usefulness of this “pulse+material” combination for high-gain ICF purposes.

References

[1] Caruso, A. and Pais, V. A., “Effects of the surface finish on the hydrodynamic evolution of surfaces exposed to thermal radiation”, Proc. of the 4^{th} Int. Workshop on the Physics of Compressible Turbulent Mixing, Cambridge, England, U. K., 20 March–1 April, 1993.

[2] Caruso, A., “High Gain Radiation-Driven Targets(I)”, Proceedings of the International School of Plasma Physics “Pietro Caldirola” on Inertial Confinement Fusion, Varenna (Italy) 6-16 September 1988, edited by A. Caruso and E. Sindoni.

[3] Caruso, A. and Pais, V. A, “High Gain Radiation-Driven Proceedings of the International School of Plasma Physics “Pietro Caldirola” on Inertial Confinement Fusion, Varenna (Italy) 6-16 September 1988, edited by A. Caruso and E. Sindoni.

[4] Caruso, A. and Pais, V. A, “Effect of surface finish on the stability of targets imploded by thermal radiation”, Proceedings of the Japan-US seminar on Physics of High Power Laser Matter Interactions, Kyoto (Japan), March 1992, in press.

[5] Caruso, A. and Pais, V. A, “Effect of surface finish on the stability of targets imploded by thermal radiation”, Laser and Particle Beams, in press.

[6] Takabe, H., et al., Phys. Fluid **28**, 3676 (1985).

[7] Lindl, J., “Introduction to the physics of ICF capsules”, Proceedings of the International School of Plasma Physics “Pietro Caldirola” on Inertial Confinement Fusion, Varenna (Italy) 6-16 September 1988, edited by A. Caruso and E. Sindoni.

[8] Nuckolls, J. et al., Nature, **239**, 139 (1972).

[9] Remington, B. A. et al., Phys. Plasmas, **2**, (1995).

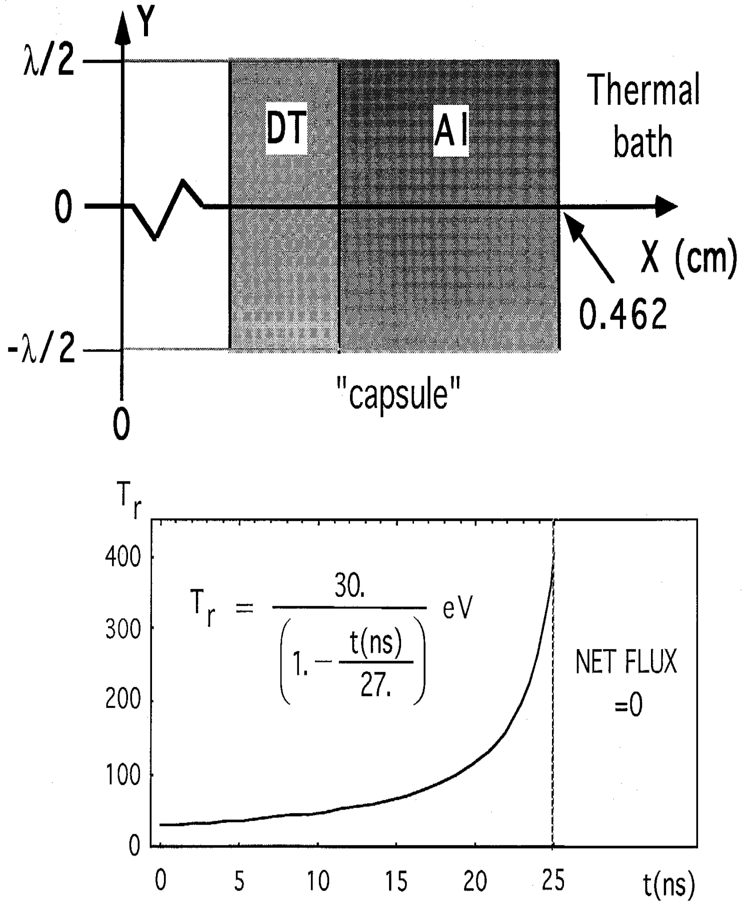

Figure 1: The planar analog for an indirectly driven, high gain thermonuclear target used in the numerical simulations.

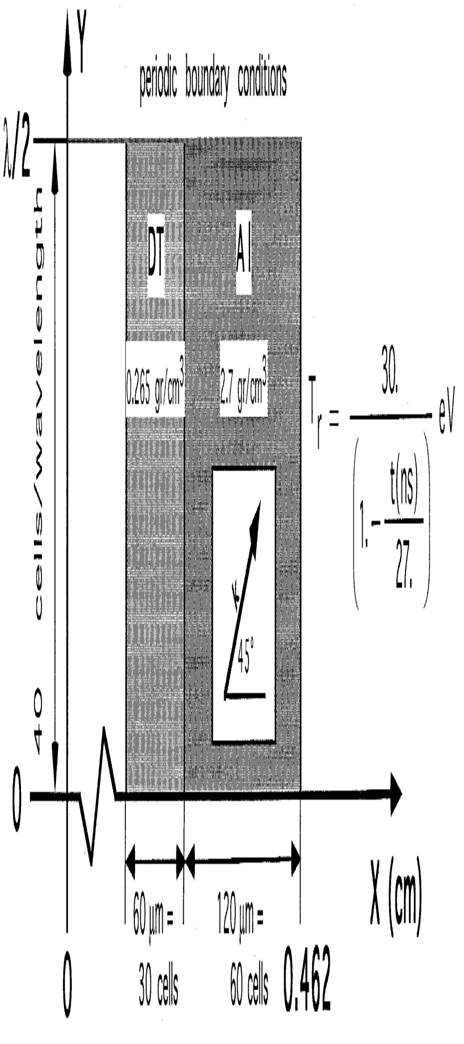

Figure 2: Schematic of the set-up used for the numerical simulations.

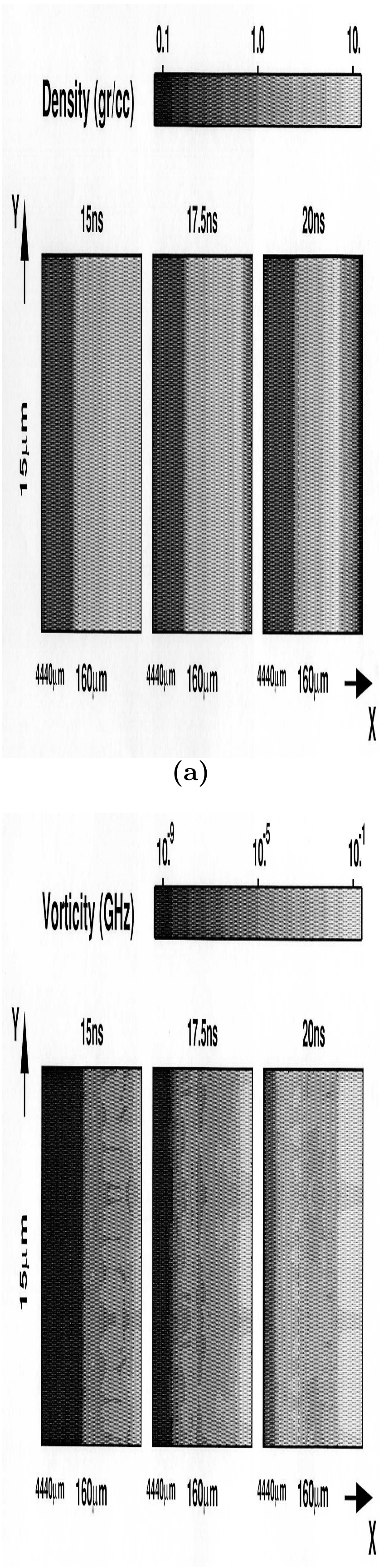

(a)

(b)

Figure 3: Transitory phase. 2D maps of the density at three different instants in the early steps of the evolution. Initial relative amplitude $\delta = 0.001$ and wavelength $\lambda = 10\mu$m. The dashed line indicates the DT-Al interface.

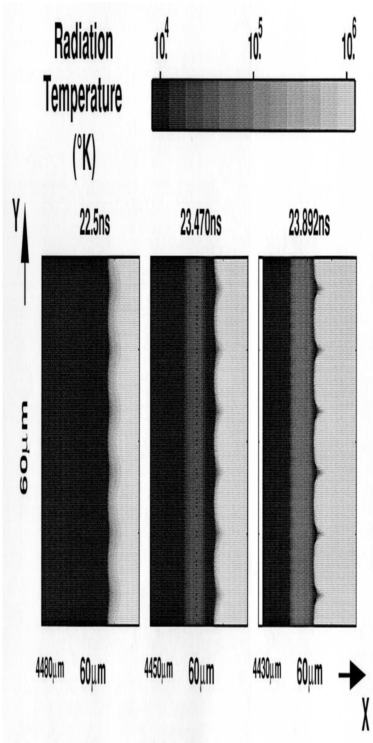
Radiation
Temperature
(°K)
10.⁴
10.⁵
10.⁶
Y
22.5ns
23.470ns
23.892ns
60µm
4480µm
60µm
4450µm
60µm
4430µm
60µm
X

(a)

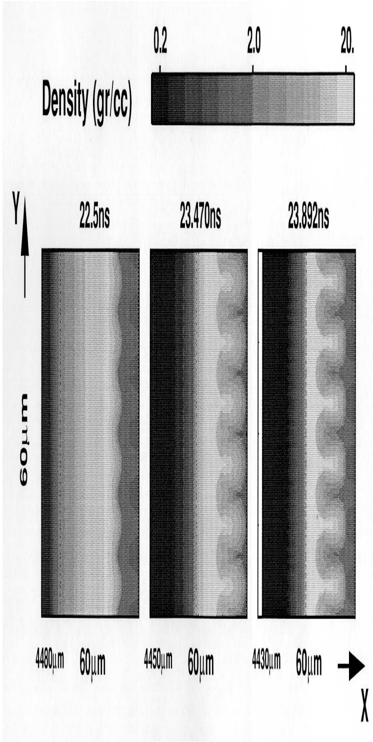
0.2
2.0
20.
Density (gr/cc)
Y
22.5ns
23.470ns
23.892ns
60µm
4480µm
60µm
4450µm
60µm
4430µm
60µm
X

(b)

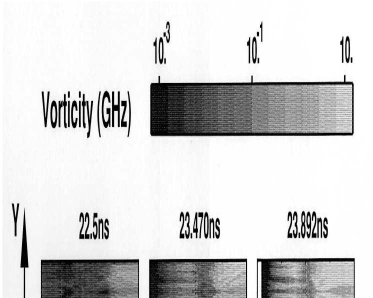
10.⁻³
10.⁻¹
10.
Vorticity (GHz)
Y
22.5ns
23.470ns
23.892ns

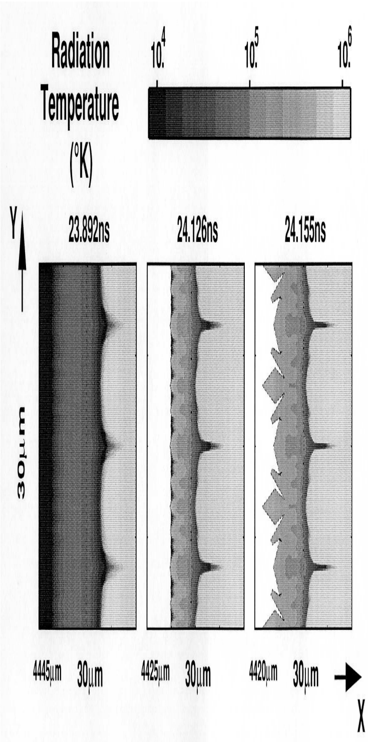
Radiation Temperature (°K)
10^4
10^5
10^6
Y
23.892ns
24.126ns
24.155ns
30µm
4445µm
30µm
4425µm
30µm
4420µm
30µm
X

(a)

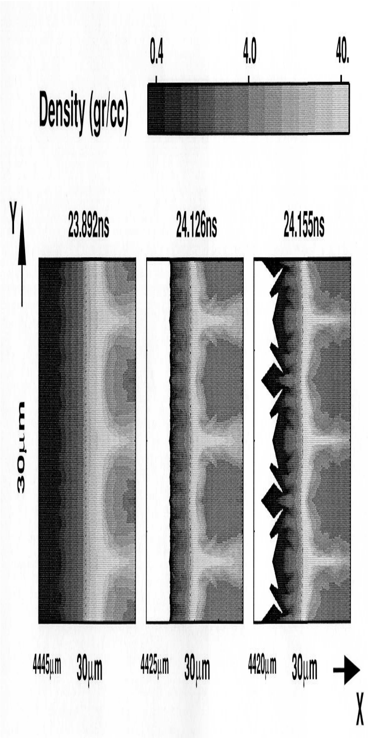
Density (gr/cc)
0.4
4.0
40.
Y
23.892ns
24.126ns
24.155ns
30µm
4445µm
30µm
4425µm
30µm
4420µm
30µm
X

(b)

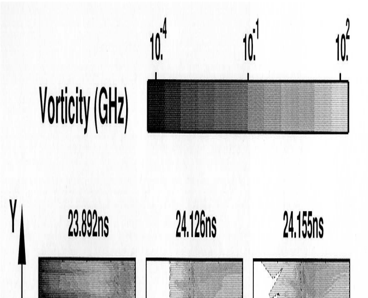
Vorticity (GHz)
10^{-4}
10^{-1}
10^2
Y
23.892ns
24.126ns
24.155ns

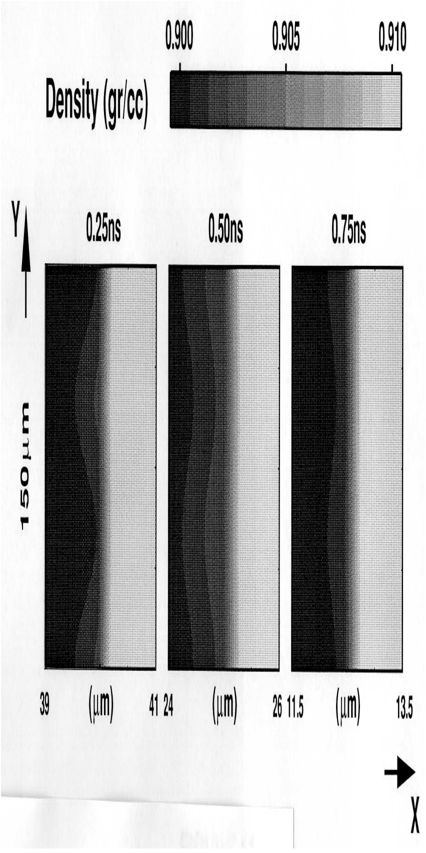

Figure 6: Evolution of the case proposed by B. A. Remington [9]. 2D maps of density at three different instants. A 50 μm width CH layer density-perturbed with initial relative amplitude $\delta = 0.001$ and wavelength $\lambda = 100\mu$m is exposed to a thermal radiation pulse as indicated in [9].